# Spin-triplet supercurrents of odd and even parity in nanostructured devices

Lahabi, K.

**Author**: Lahabi, K.
**Title**: Spin-triplet supercurrents of odd and even parity in nanostructured devices
**Issue Date**: 2018-12-04

# 2

# Pairing symmetry

## 2.1. General symmetry classes

In a superconducting material, Cooper pairs can form at the Fermi surface by some type of weakly attractive interaction. The origin of this attractive interaction however, appears to vary for different types of superconductors. For instance, it is more or less established that in most elemental superconductors (e.g. Al, Pb and Nb) the electron-phonon coupling is responsible for the pair formation. This class of material are generally referred to as conventional or BCS superconductors, as they can be described by the BCS theory. This theory however fails to describe a growing number of so-called "unconventional" superconductors, including cuprates and heavy fermions. While the exact origin of unconventional superconductivity is currently not clear, it is however evident that the pairing mechanism is more closely related to spin fluctuations than BCS-type electron-phonon coupling. A discussion on these interactions would go well beyond the scope of this thesis. Instead, here we focus on the different types of wavefunction which, at least in principle, could allow two electrons to exist as a pair, irrespective of the underlying interactions involved.

The superconducting wavefunction is generally represented by a complex gap function $\Delta$. This corresponds to the energy gap which develops around the Fermi surface when electrons are condensing into Cooper pairs — illustrated in Figure 2.1. Within this gap electrons are in a coherent state, and are only available as Cooper pairs. The size of the gap is a measure of the energy of a condensate, as it roughly translates to the energy required to break a pair by exciting electrons (holes) to states above

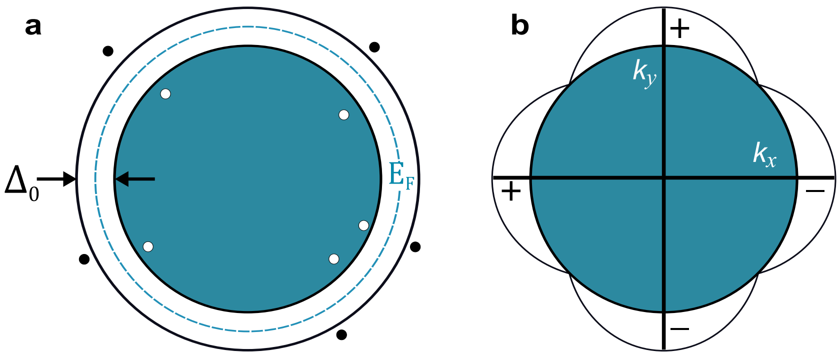


Figure 2.1: The superconducting gap. **a** Representation of a BCS superconductor. Pairing occurs within a uniform energy gap formed around the Fermi surface $E_F$ (the shaded region represents occupied electron states). Unpaired electrons (black dots) and holes (white dots) are not allowed within the gap. They only appear as quasiparticles in the states above and below the gap. BCS superconductors are characterised by an isotropic gap $\Delta_0$, uniform in $k$-space. **b** The $d_{x^2-y^2}$ gap, common amongst cuprates. The order parameter consists of four lobes with alternating phase (represented by+/−). This leads to an anisotropic gap which goes to zero in certain directions (here, along $k_\mathrm{x} = \pm k_\mathrm{y}$).

(below) the superconducting gap. It is important to remember that the gap function is essentially the wavefunction of two electrons in a paired state which, broadly speaking, behaves as a Bose particle. Nevertheless, the constituting electrons are still fermions; and therefore must preserve the anticommuting properties that follow from the Pauli exclusion principle. This, in a nutshell, means that a paired state between two fermions is only allowed if its wavefunction is antisymmetric i.e. changes sign upon exchange of particles. This condition can be satisfied in a number of ways, as there are three distinct components in the wavefunction of a pair of electrons. These are spin, space (represented by the orbital part of the wavefunction in momentum space) and time (or frequency). Each component is allowed to correspond to an odd or even function. However, the *overall* wavefunction (the product of all three) must always be odd.

Cooper pairs can be divided into two categories based on their spin symmetry: singlets (odd) and triplets (even). For the singlet $(|\uparrow\downarrow\rangle - |\downarrow\uparrow\rangle)/\sqrt{2}$, the sum of the spin angular momenta is zero ($S = 0$), while the combined spin of a triplet pair is $S = 1$. There are three distinct triplet states with different spin projections ($m_s$) defined with respect to the quantization axis for spin. These are $|\uparrow\uparrow\rangle$; ($m_s = 1$), $|\downarrow\downarrow\rangle$; ($m_s = -1$) and $(|\uparrow\downarrow\rangle + |\downarrow\uparrow\rangle)/\sqrt{2}$; ($m = 0$). The first two correspond to equal-spin pairing, where the electron spins are parallel to each other.

With respect to the momentum (spatial) symmetry, it is customary to implement the conventions used in describing atomic orbitals. Depending on its orbital component

($L$), the symmetry of the order parameter can be approximated by the shape of the $s$ ($L = 0$), $p$ ($L = 1$), $d$ ($L = 2$) and $f$ ($L = 3$) orbitals. Superconductors with $s$- or $d$-wave gaps are momentum-symmetric (even-parity), while the $p$- and $f$-wave gaps are represented by pair functions with an antisymmetric momentum (odd-parity). A BCS superconductor is characterised by $s$-wave symmetry. This corresponds to an isotropic order parameter in $k$-space (see Figure 2.1**a**), with a uniform gap around the Fermi surface $\Delta(\mathbf{k}) = \Delta_0$ (independent of $k$). Cuprates on the other hand (e.g. YBCO), are mostly characterised by the $d$-wave order parameter $d_{x^2-y^2}$, shown in Figure 2.1**b**. Such a gap is anisotropic with respect to the Fermi sheet, and its amplitude and phase are both $k$-dependent. More specifically, $\Delta(\mathbf{k})$ is represented by four lobes with alternating (reversed) phase. This also results in nodes in the superconducting gap, where the parameter is suppressed along certain axes.[1]

While frequency symmetry may seem as an abstract concept, which can only be expressed in terms of the Gor'kov anomalous Green function [2] in the Matsubara representation [3], its basic idea can be readily understood by picturing the correlation between two electrons as a function of time. The restrictions of the Pauli principle are imposed to this correlation at equal *times*. This means the two electrons cannot occupy the same state at the same time. The electrons however can avoid each other through the exchange of time variables. This corresponds to a pair function with asymmetric (odd) time component. Naively, one can think of this as a form of quantum mechanical timesharing, where two electrons can occupy the same state at different times. The time component of the correlation function is conveniently represented by a Matsubara frequency $\omega$. An order parameter has odd-frequency if $\Delta(-\omega) = -\Delta(\omega)$.

Given that the overall pairing function must be antisymmetric, we can combine the symmetries of spin, frequency and momentum components to represent the allowed pairings states; compatible with the exclusion principle and Fermi-Dirac statistics. All Cooper pairs now can be categorised into four general groups, shown in Figure 2.2. This classification scheme was formalised independently by Eschrig *et al.* [4], and by Tanaka and Golubov [5, 6] in 2007.

Spin singlet Cooper pairs can either occur with even-frequency and even-parity, or with odd-frequency and odd-parity. These correspond to the first and second categories of Figure 2.2 respectively. Remarkably, the first category alone represents the overwhelming majority of all known superconductors. This includes all BCS superconductors ($s$-wave) as well as high-$T_c$ cuprates and a large number of other unconventional superconductors with $d$-wave symmetry.

[1] Note that in some literature a $k$-dependent order parameter is considered as the criterion for unconventional superconductivity (e.g. Ref [1]) This classification however tends to neglect $s$-wave odd-frequency triplets and signed-reversed $s$-wave pairing, predicted for iron pnictides, by grouping them together with conventional (BCS-like) singlets.

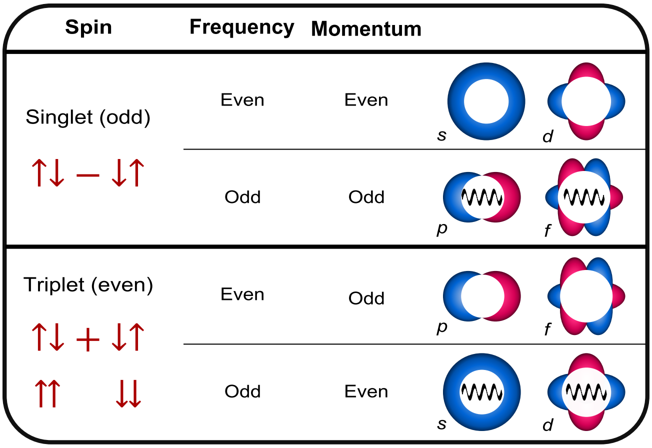


Figure 2.2: The four classes of Cooper pair symmetry, as allowed by the Pauli principle. This classification is based on three independent components which determine the overall pairing symmetry of the superconducting wavefunction: spin, frequency and momentum. The drawings in the right panel represent the allowed orbital symmetries for each category. The black wavy line represents odd frequency.

The available symmetries for spin triplet Cooper pairs are represented in the third and fourth classes of Figure 2.2: even-frequency with odd-parity; and odd-frequency even-parity respectively. The former category was first discovered in the $p$-wave superfluid that forms in $^3$He [7], and is also the proposed symmetry for the superconducting phase that occurs in $Sr_2RuO_4$ below 1.5 K.

The last category of triplets was intitially introduced by in 1974 by Berezinskiĭ [8] as a proposal for superfluidity in $^3$He, which later was found to be $p$-wave instead. While an odd-frequency triplet state has so far never been observed by itself in nature, it was found that its pairing amplitude can be generated at (carefully engineered) superconductor-ferromagnet (S-F) interfaces [9, 10]. The triplet correlations studied in our S-F hybrids correspond to odd-frequency with $s$-wave symmetry.

Odd-frequency triplet pairing can be realised with a simple $s$-wave gap. This has a profound consequence on the survival of these correlations in a diffusive environment, where strong scattering leads to the mixing of different $k$ states, see Figure 2.3. A $p$-wave gap, characterised by a $k$-dependent phase, would be fully suppressed under strong averaging in $k$-space. The $s$-wave gap on the other hand, is protected from scattering by its $k$-independent phase. As a consequence, the (odd-frequency) $s$-wave triplet pairing can be realised in a variety of diffusive S-F hybrids, made from a wide range of materials. In contrast, odd-parity (*e.g.* $p$-wave) triplet correlations are characterised by the clean limit (i.e. non-diffusive), and are restricted to a rather small number of materials, amongst which, $Sr_2RuO_4$ is one of the most prominent candidates (for a review see Refs. [11]). In this particular case, the order parameter

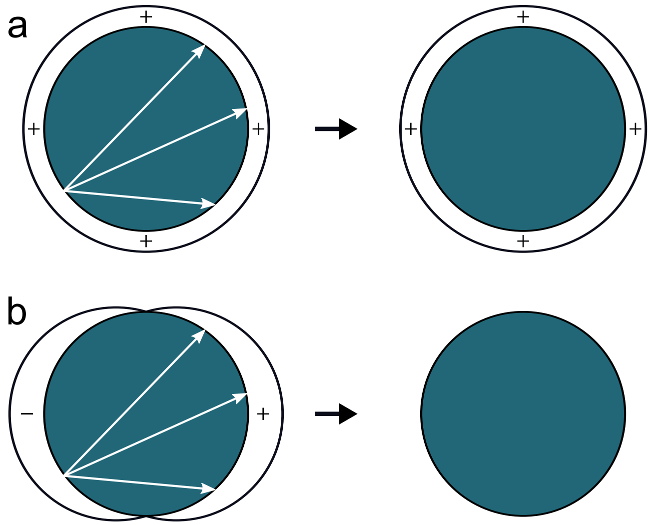


Figure 2.3: Representation of elastic scattering for two different order parameters. Each case shows the phase (denoted by +/−) and amplitude of the superconducting gap with respect to the Fermi surface (shaded). The arrows in the left panel represent typical elastic scattering events. The effect of scattering on the order parameter is shown in the right panel. **a**, The *s*-wave gap corresponds to an isotropic gap, where phase and amplitude are $k$-independent. The order parameter is practically unaffected under strong scattering. **b**, The *p*-wave order parameter is characterized by a $k$-dependent phase. As a result, the gap is averaged to zero by the scattering events — leading to a complete loss of superconductivity

is expected to be of $p_x \pm i p_y$ form, which can be considered as the two-dimensional analogue of the A-phase of superfluid $^3$He.

## 2.2. PAIRING SYMMETRY OF $Sr_2RuO_4$

This section introduces the general formalism used to describe odd-parity symmetry, with an emphasis on *p*-wave pairing and its significance in the context of $Sr_2RuO_4$. This subject can be better appreciated with some background on the material.

### 2.2.1. $Sr_2RuO_4$: BASIC PROPERTIES

Since its discovery in 1994 by Maeno *et al.* [12], the superconducting state in $Sr_2RuO_4$ has been the subject of thousands of studies. Yet, to this date, the symmetry of its order parameter remains a moot point, making this material one of the most controversial superconductors.

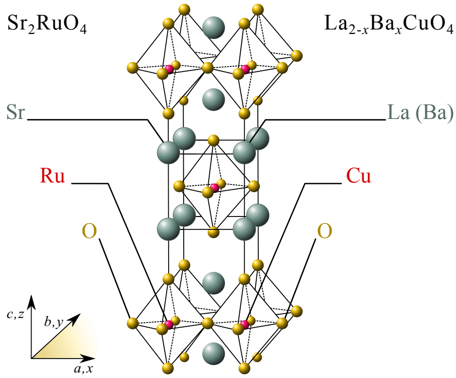


Figure 2.4: $Sr_2RuO_4$ (left) has a common layered perovskite structure with cuprate superconductors such as $La_{2-x}Ba_xCuO_4$ (right).

Table 2.1: Superconducting parameters of $Sr_2RuO_4$. $H_c$ and $H_{c2}$ are the thermodynamic and upper critical fields, respectively, $\xi$ is the coherence length and $\lambda$ is the magnetic penetration depth. The values are taken after Ref. [11].

| Parameter | | | $ab$ | $c$ |
|---|---|---|---|---|
| $T_c$ | [K] | 1.5 | | |
| $\mu_0 H_c$ | [T] | 0.023 | | |
| $\mu_0 H_{c2}$ | [T] | | 1.5 | 0.075 |
| $\xi(0)$ | [nm] | | 66 | 3.3 |
| $\lambda(0)$ | [nm] | | 190 | 3000 |

As shown in Figure 2.4, $Sr_2RuO_4$ has the same lattice structure as the high $T_c$ cuprates such as $La_{2-x}Ba_xCuO_4$; but only becomes superconducting below 1.5 K. More importantly, unlike $La_2CuO_4$, which is an antiferromagnetic insulator, $Sr_2RuO_4$ is highly metallic with a (quasi) 2-dimensional Fermi surface consisting of three cylindrical sheets. This is also evident in the pronounced ratio of out-of-plane to in-plane resistivity ($\rho_c/\rho_{ab} > 1400$ at low temperatures) [13]. $Sr_2RuO_4$ is also highly anisotropic as a superconductor. As shown in Table 2.1, the in-plane to out-of-plane coherence lengths correspond to an anisotropy ratio of 20. However, $\xi_c$ is still several times larger than the interlayer spacing (12.72 Å), allowing interlayer coherence.

In direct contrast to cuprates, normal state $Sr_2RuO_4$ can be well described as a (quasi) 2-dimensional Landau-Fermi liquid, with a distinct $T^2$ dependence of resistivity at low temperatures [14]. In fact the superconducting transition at 1.5 K only occurs in exceptionally clean crystals, with residual resistivities below $1\mu\Omega$cm at low temperatures, corresponding to an electron mean free path of $l \approx 1-3$ $\mu$m [15]. The superconducting state is also highly vulnerable to nonmagnetic impurities. It was found that even trace amounts of Al and Si ($\approx$ 400 ppm) are sufficient to fully suppress $T_c$. As described in Section 2.1, such pronounced sensitivity to elastic scattering is a hallmark of unconventional superconductivity – where the order parameter has a $k$-dependent phase (see Figure 2.3).

Given the Landau-Fermi liquid behaviour; and the results of de Haas-van Alphen experiments — which show an enhancement of the effective mass by a factor of 3-5 [16] — it is also evident that the relevant interactions at low temperatures are predominantly due to strongly correlated electrons (as opposed to weak electron-phonon interactions). As first indicated by Sigrist and Rice (1995) [17], these characteristics bear an uncanny resemblance with that of $^3$He, which also is a well-characterised

Landau-Fermi liquid. Based on this, and the close affinity with ferromagnetic oxides such as $SrRuO_3$, the authors proposed that $Sr_2RuO_4$ may have a triplet pairing — similar to that of the $p$-wave superfluid $^3$He.

By now there is a substantial body of experimental evidence supporting the equal-spin triplet pairing in $Sr_2RuO_4$. These include NMR Knight-shift [18] and polarized neutron measurements [19], observation of half-quantum vortices [20, 21] (see Chapter 6) and the experiments on $Sr_2RuO_4$-ferromagnet hybrids [22]. The orbital parity of $Sr_2RuO_4$ however has been far more challenging to establish, and remains a highly debated subject.

### 2.2.2. $d$-VECTOR FORMALISM

Unlike for even-parity (i.e. $s-$ or $d$-wave pairing), a $p$-wave gap breaks the reflection symmetry of a 2-dimensional square lattice. Moreover, triplet pairing requires three independent gap functions to describe the spin symmetry. This can be represented by a general $2 \times 2$ gap matrix in momentum space.

$$\Delta(\boldsymbol{k}) = \begin{pmatrix} \Delta_{\boldsymbol{k},\uparrow\uparrow} & \Delta_{\boldsymbol{k},\uparrow\downarrow} \\ \Delta_{\boldsymbol{k},\downarrow\uparrow} & \Delta_{\boldsymbol{k},\downarrow\downarrow} \end{pmatrix} \tag{2.1}$$

For a given quantization direction, $\Delta_{\uparrow\uparrow}$ and $\Delta_{\downarrow\downarrow}$ represent spin projections of $+1$ and $-1$, respectively, while $\Delta_{\uparrow\downarrow} = \Delta_{\downarrow\uparrow} = \Delta_0$ corresponds to triplet pairing with zero spin projection (i.e. Cooper pairs do have a spin $S = 1$, but it lies perpendicular to the quantization axis). This gap matrix can be elegantly reduced to a three-dimensional complex vector $\boldsymbol{d}(\boldsymbol{k}) = [d_x(\boldsymbol{k}), d_y(\boldsymbol{k}), d_z(\boldsymbol{k})]$ (known as the $d$-vector), defined by

$$\begin{pmatrix} \Delta_{\boldsymbol{k},\uparrow\uparrow} & \Delta_{\boldsymbol{k},0} \\ \Delta_{\boldsymbol{k},0} & \Delta_{\boldsymbol{k},\downarrow\downarrow} \end{pmatrix} = \begin{pmatrix} -d_x(\boldsymbol{k}) + i d_y(\boldsymbol{k}) & d_z(\boldsymbol{k}) \\ d_z(\boldsymbol{k}) & d_x(\boldsymbol{k}) + i d_y(\boldsymbol{k}) \end{pmatrix} \tag{2.2}$$

A state is called unitary if $\left|\boldsymbol{d}(\boldsymbol{k}) \times \boldsymbol{d}^*(\boldsymbol{k})\right| = 0$. In this case, $\boldsymbol{d}(\boldsymbol{k})$ has a straightforward meaning: its amplitude is proportional to size of the gap at $(\boldsymbol{k}, -\boldsymbol{k})$; and its direction is perpendicular to the plane of equal-spin paired electrons, where $|\uparrow\uparrow\rangle$ and $|\downarrow\downarrow\rangle$ can be defined with respect to any quantization direction in that plane. For instance, if we choose $z$ to be the quantization axis for spin, then the $d$-vector $\boldsymbol{d}(\boldsymbol{k}) = [0, 0, d_z(\boldsymbol{k})] \parallel \hat{\mathbf{z}}$ would correspond to $\Delta_{\uparrow\uparrow z} = \Delta_{\downarrow\downarrow z} = 0$. This only leaves $\Delta_{0z}$, which means the Cooper pair spins must lie perpendicular to the quantization axis (i.e. in the $xy$ plane $\perp \boldsymbol{d}$).

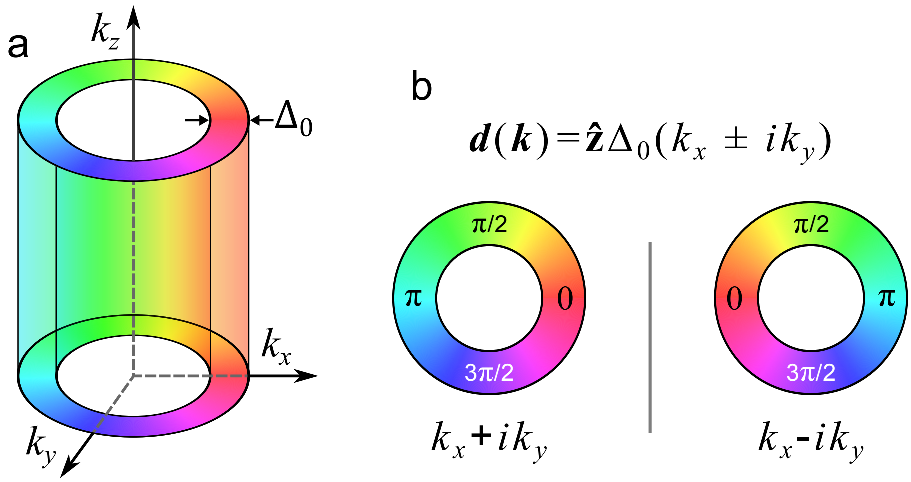


Figure 2.5: Energy gap of the chiral $p$-wave state $\boldsymbol{d}(\boldsymbol{k}) = \hat{\mathbf{z}}\Delta_0(k_x \pm ik_y)$. Colours represent the orbital phase of the order parameter $\theta_k$, where $\boldsymbol{d}(\boldsymbol{k}) \propto e^{i\theta_k}$. (**a**) The two-dimensional gap forms around the cylindrical Fermi surface. While the gap amplitude $\Delta_0$ is isotropic in the $xy$ plane, its phase varies continuously. (**b**) The degenerate "chiral" states $k_x - ik_y$ and $k_x + ik_y$ wind their phase in opposite directions.

If we switch the quantization axis from $z$ to any direction along the $xy$ plane, there would be equal densities of $|\uparrow\uparrow\rangle$ and $|\downarrow\downarrow\rangle$ Cooper pairs with spin projections of +1 and −1, corresponding to zero spin polarization for the condensate. The absence of spin polarization is a common characteristic of all unitary states, since $|\Delta_{\uparrow\uparrow}|^2 - |\Delta_{\downarrow\downarrow}|^2 = 2i[\boldsymbol{d}(\boldsymbol{k}) \times \boldsymbol{d}^*(\boldsymbol{k})]_z = 0$.

In the absence of external fields, unitary states are more applicable (than nonunitary states) to $Sr_2RuO_4$. A list of possible unitary states for a tetragonal lattice with a cylindrical Fermi surface (appropriate for $Sr_2RuO_4$) is presented in Table 2.2. Amongst these, the $\boldsymbol{d}(\boldsymbol{k}) \propto \hat{\mathbf{z}}(k_x \pm ik_y)$ state is the most discussed pairing symmetry in the context of $Sr_2RuO_4$. In this case the $d$-vector is weakly pinned to the $c$-axis of the lattice ($z \parallel c$), and corresponds to a full (isotropic) gap in the $ab$ plane (see Figure 2.5).

The order parameter has a $k$-dependent phase (represented by colours), which continuously winds in 2 dimensions as a function of $k_x$ and $k_y$ (i.e. in the $ab$ plane). Since the order parameter can wind its phase in either directions, it results in two degenerate states $k_x + ik_y$ and $k_x - ik_y$ with opposite phase windings. This superconducting state $\boldsymbol{d}(\boldsymbol{k}) \propto e^{i\theta_k}$ is therefore characterised by an orbital phase $\theta_k$ which has a direction (i.e. winding left or right).

The direction of $\theta_k$ is considered as the "chirality" of the superconducting state, and is responsible for the broken time-reversal symmetry (TRS) associated with this order parameter. A bulk crystal of $Sr_2RuO_4$ is expected to spontaneously break into a

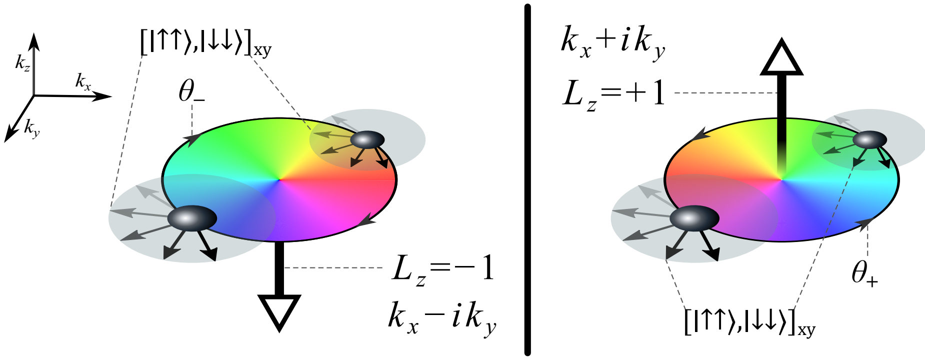


Figure 2.6: Chiral Cooper pairs of $k_x - ik_y$ and $k_x + ik_y$ states. Small arrows represent equal-spin pairing of the electrons. Spin quantization axis is defined as *any* direction in the $xy$ plane, resulting in zero spin polarization. Both chiral states have the same spin symmetry. Colours correspond to the orbital phase $\theta$, which has a different winding direction in each state, hence the ± sign. Large arrows represent the orbital angular momentum of each Cooper pair, which is responsible for breaking the time-reversal symmetry.

multitude of spatially segregated *domains* of $k_x + ik_y$ and $k_x - ik_y$ chirality. However, if a system is sufficiently small and homogenous, it can also be in a single domain state. This means that, when cooled below $T_c$, one of the chiral states will spontaneously emerge over the entire superconductor.

As shown in Figure 2.6, Cooper pairs consist of equal-spin electrons with a total spin $S = 1$, which lies in the *ab* plane. However, $|\uparrow\uparrow\rangle$ and $|\downarrow\downarrow\rangle$ states have equal weights along *any* given quantization axis in the *ab* plane. While $|\uparrow\uparrow\rangle$ and $|\downarrow\downarrow\rangle$ each have a spin projection ($S_{xy} = \pm 1$), the total spin polarization is zero. In the absence of external fields, this can be thought of as the superposition of $|\uparrow\uparrow\rangle$ and $|\downarrow\downarrow\rangle$ states. Also note that both chiralities have the same spin symmetry i.e. $k_x + ik_y$ and $k_x - ik_y$ cannot be distinguished by the spin part of the order parameter.

Generally, a $p$-wave orbital would automatically imply an orbital angular momentum $L = 1$. For $k_x \pm ik_y$ states, this would correspond to $L_z = \pm 1$. This means that the electrons of a Cooper pair have a relative orbital motion, which depends on chirality (the pairs are rotating either clockwise or anticlockwise). The direction of orbital motion, and therefore the sign of $L_z$, is determined by the winding direction of the orbital phase $\theta_k$ (represented by $\theta_-$ and $\theta_+$ in Figure 2.6). The fact that within each chiral state *all* electron pairs have the same rotation (either clockwise or anticlockwise) breaks the TRS. Unlike the non-unitary states, which break TRS by having a preference of one of the spins, here TRS breaking is purely due to the orbital part of the wavefunction.

An important consequence of this would be the emergence of the so-called *edge current*, which refers to a finite charge current at the boundaries of a single chiral domain. Even in the absence of external fields, the edge current would spontaneously appear at the onset of $T_c$ and its direction is purely defined by the intrinsic direction of the orbital phase – and hence chirality.

### 2.2.3. POSSIBLE SYMMETRIES FOR $Sr_2RuO_4$

Our discussion on parity has so far been focused on the $k_x \pm ik_y$ state, while we conveniently ignored the other symmetry candidates for $Sr_2RuO_4$ . Table 2.2 lists all the unitary states with a $p$-symmetry for a tetragonal crystal with a cylindrical Fermi surface (labelled **A** to **G**). The derivations can be found in Refs. [17, 23, 24] The following discussion intends to compare the likelihood of the listed symmetries by examining the results of a number of key experiments. For a more detailed review on this topic, the reader is refered to Refs. [1, 11, 25].

We can divide the items of Table 2.2 into two groups based on orientation of the $d$-vector. In the first category (**A—D**), the $d$-vector has an arbitrary orientation in the $ab$ plane. This means that the spin of the Cooper pairs must be aligned with $c$ axis ($d$-vector points perpendicular to Cooper pair spin). For the second category (**E—G**), which also includes the previously mentioned $k_x \pm ik_y$ case, the $d$-vector has a well-defined direction, pointing along the $c$-axis. Hence, the Cooper pairs have spins that lie in the $ab$ plane (as we saw for $k_x \pm ik_y$). The two categories can therefore be distinguished by the spin part of the order parameter. This can be investigated by measuring the spin susceptibility in the presence of an external magnetic field. For instance, if there is sufficient spin-orbit coupling to pin the $d$-vector to the lattice, which is the case for (**E—G**), then the measured spin susceptibility would depend on the direction of the $d$-vector.

Under a constant applied field, the spin susceptibility of a singlet superconductor $S = 0$ would simply begin to drop when cooled down below $T_c$. For a triplet superconductor however the situation is considerably different. If the external field is along the plane of equal-spin paired electrons ($H \perp \boldsymbol{d}$), it would induce a spin polarization by creating an imbalance between the population of $\uparrow\uparrow$ and $\downarrow\downarrow$ states. By contrast, if $H \parallel \boldsymbol{d}$ the spins of the Cooper pairs will lie in a perpendicular plane to the applied field, and the condensate cannot be polarized.

The spin susceptibility of $Sr_2RuO_4$ has been measured by a number of independent techniques, including Knight shift experiments [18] and polarized neutron scattering [19]. These studies have consistently found that, if a field is applied along the $ab$ plane, the spin susceptibility remains unchanged by the superconducting transition (i.e. same susceptibility signal above and below $T_c$).

There are two aspects to the significance of these observations. First, they provide

| $d$-vector | $\Delta/\Delta_0$ | direction | TRS | Label |
|---|---|---|---|---|
| $\hat{\mathbf{x}}k_x + \hat{\mathbf{y}}k_y$ | $\sqrt{k_x^2+k_y^2}$ | $\boldsymbol{d}\parallel ab$ | preserved | **A** |
| $\hat{\mathbf{x}}k_y - \hat{\mathbf{y}}k_x$ | $\sqrt{k_x^2+k_y^2}$ | $\boldsymbol{d}\parallel ab$ | preserved | **B** |
| $\hat{\mathbf{x}}k_x - \hat{\mathbf{y}}k_y$ | $\sqrt{k_x^2+k_y^2}$ | $\boldsymbol{d}\parallel ab$ | preserved | **C** |
| $\hat{\mathbf{x}}k_y + \hat{\mathbf{y}}k_x$ | $\sqrt{k_x^2+k_y^2}$ | $\boldsymbol{d}\parallel ab$ | preserved | **D** |
| $\hat{\mathbf{z}}k_x$ | $\lvert k_x\rvert$ | $\boldsymbol{d}\parallel c$ | preserved | **E** |
| $\hat{\mathbf{z}}(k_x + k_y)$ | $\lvert k_x + k_y\rvert$ | $\boldsymbol{d}\parallel c$ | preserved | **F** |
| $\hat{\mathbf{z}}(k_x \pm ik_y)$ | $\sqrt{k_x^2+k_y^2}$ | $\boldsymbol{d}\parallel c$ | broken | **G** |

Table 2.2: List of possible unitary states with $p$-wave symmetry for $Sr_2RuO_4$ [1].

strong evidence in favour of triplet pairing in $Sr_2RuO_4$, due to the measured spin polarization below $T_c$. The second is that the same behaviour is observed for different directions in the $ab$ plane, which suggests a uniform $d$-vector pointing along the $c$ axis. This is in agreement with our second category (**E—G**), and $\hat{\mathbf{z}}(k_x \pm ik_y)$ in particular, since the amplitude of $\boldsymbol{d}$ does not have a $\boldsymbol{k}_{x,y}$ dependence (i.e. the gap is homogenous in the $ab$ plane). However, these measurements still cannot conclusively prove that the $d$-vector is pinned to the $c$-axis. The uncertainty comes from the fact that a $d$-vector with no specific relation to the crystal (uniform in all 3-dimensions), could presumably also change its orientation under the applied field and yield a similar results. One solution to this would be to measure the spin susceptibility with $H \parallel c$. Since the spins should then be in the plane that is perpendicular to the applied field, one would expect to find no spin polarization. Such experiments however have proven rather challenging due to the large anisotropy of the superconductor, which requires the applied field to be 20 times smaller than the ones used for the $ab$ plane (see Table 2.1).

In summary, based on spin-susceptibility measurements, an order parameter with $\boldsymbol{d} \parallel c$ (i.e. $|\uparrow\uparrow\rangle, |\downarrow\downarrow\rangle \parallel ab$), seems quite probable for $Sr_2RuO_4$. Amongst the three order parameters with $\boldsymbol{d} \parallel c$, only $\hat{\mathbf{z}}(k_x \pm ik_y)$ corresponds to a full gap in the $ab$ plane. Both $\hat{\mathbf{z}}k_x$ and $\hat{\mathbf{z}}(k_x + k_y)$ cases (**E** and **F**) are associated with vertical line nodes. So far however, no evidence of such vertical line nodes has been found, making the relevance of **E** and **F** somewhat harder to justify.

Arguably, the most unique characteristic of a chiral order parameter is the breaking of time-reversal symmetry (TRS). This fundamental distinction can already be deduced from the list of $d$-vectors in Table 2.2, where $\hat{\mathbf{z}}(k_x \pm ik_y)$ is the only one with broken TRS. The reason for this can be understood by examining how TRS is restored in a number of examples. For instance, consider $\hat{\mathbf{x}}k_x + \hat{\mathbf{y}}k_y$ (state **A**), which can also be written as

$$\hat{\mathbf{x}}k_x + \hat{\mathbf{y}}k_y = \frac{1}{2}\Big[\overbrace{(\hat{\mathbf{x}} + i\hat{\mathbf{y}})}^{S_z=+1}\underbrace{(k_x - ik_y)}_{L_z=-1} + \overbrace{(\hat{\mathbf{x}} - i\hat{\mathbf{y}})}^{S_z=-1}\underbrace{(k_x + ik_y)}_{L_z=+1}\Big] \tag{2.3}$$

which is the superposition of two states with opposite spin ($\hat{\mathbf{x}} \pm i\hat{\mathbf{y}}$) and orbital ($k_x \pm ik_y$) components. Each state has a spin ($S_z$) and orbital angular momentum ($L_z$). They are both quantized along the $c$-axis, and are antiparallel to each other (i.e. $S_z = \mp 1$ corresponds to $L_z = \pm 1$). When the two states are combined however, the resulting $L$ and $S$ are both zero, and TRS is therefore respected.

A more similar example to the chiral $d$-vector $\hat{\mathbf{z}}(k_x \pm ik_y)$ would be $\hat{\mathbf{z}}k_x$ (state **E**), as it also has a direction along $c$ — with the spin plane $(|\uparrow\uparrow\rangle, |\downarrow\downarrow\rangle)_{xy} \parallel ab$. This can be represented as

$$\hat{\mathbf{z}}k_x = \frac{1}{2}\hat{\mathbf{z}}\Big[\overbrace{(k_x + ik_y)}^{L_z=+1} + \underbrace{(k_x - ik_y)}_{L_z=-1}\Big] \tag{2.4}$$

This can be considered as the superposition of two states with equal and opposite angular momenta. The spin of each state is characterized by the equal population of $|\uparrow\uparrow\rangle$ and $|\downarrow\downarrow\rangle$ pairs, defined with respect to any quantization axis along the *ab* plane. Consequently, this order parameter cannot be assigned with a net value for either $L$ or $S$, which means that TRS is once again respected.

The order parameter of $\hat{\mathbf{z}}(k_x \pm ik_y)$ is the only $p$-wave unitary state which spontaneously breaks TRS with its orbital part. This implies that each chiral state will have a finite magnetization, even in the absence of external magnetic fields. There are currently two independent experiments which strongly support this claim. The first evidence of TRS breaking came from muon spin-relaxation ($\mu$SR) measurements, which showed the spontaneous appearance of an *internal* magnetic field below the superconducting transition temperature [26]. In this technique, 100 % spin-polarized muons are implanted (one at the time) into a material over a finite depth. The muon spin then begins to evolve in presence of the *local* magnetic fields at its implantation site. Subsequently, when the muon decays ($\approx 2.2$ $\mu$s), a positron is emitted in a direction that corresponds to the spin of the muon at the time of its decay. Hence, each muon acts as a local magnetic probe for its immediate environment. A typical experiment is based on measuring $10^7$ individual events.

In the absence of external magnetic fields the muon measurements found a dilute distribution of internal magnetic fields. This is a direct indication of TRS breaking, and also supports the existence of chiral domains, where the edge currents of individual domains can results in local magnetic fields *inside* the superconductor. Given the finite size of the domains, and their arbitrary arrangements in a three-dimensional sample, it is reasonable that the internal fields would be heavily diluted and smeared out. This makes $\mu$SR a particularly powerful technique, since a muon can directly probe the local magnetic fields of its immediate environment. While $\mu$SR serves as a reliable test for TRS — which would ultimately be in favour of the chiral order parameter — the measurements cannot conclusively prove that the internal magnetic fields of $Sr_2RuO_4$ are necessarily produced by chirality.

The breaking of TRS in $Sr_2RuO_4$ has also been confirmed by ultra-high resolution magneto-optic polar Kerr effect (PKE) measurements [27]. This technique is related to the magneto-optic Kerr effect (MOKE), where the polarization direction of a polarized light beam is rotated upon being reflected from a magnetic surface. The PKE experiments found a rotation of the polarization plane of the light reflected from the *ab* plane of the crystal. This rotation corresponded to a Kerr signal of the order of $10^{-9}$ rad. It appears spontaneously at $T_c \approx 1.5$ K and increases in magnitude by lowering the temperature down to 0.5 K, where it seems to saturate at $60 \times 10^{-9}$ rad. While this Kerr signal may seem small, it is still well within the exceptionally high resolution of the measurement apparatus (see Ref. [28] for more details).

In the absence of external fields, the sign of the Kerr signal randomly switches with each cooling cycle. The sign of the signal may indeed correspond to the orbital angular momentum of a chiral domain. In that case, the chirality of the area probed with the beam would be naturally non-deterministic, switching randomly with each cooling cycle. More importantly, it was shown that the sign of the Kerr signal can be reversed by field cooling ($\gtrsim 5$ mT) the sample prior to the (zero field) PKE measurements. It has been proposed that applying a magnetic field whilst cooling through $T_c$, can promote one chirality over the other. The field is expected to enhance the size of the domains whose angular momentum has the same direction as the applied field [29].

To this date, the results of the PKE experiments provide one of the most compelling arguments in favour of the chiral order parameter in $Sr_2RuO_4$. In addition to demonstrating TRS breaking, the PKE measurements indicate that the condensate may be divided into domains with opposite magnetic signs, along the *ab* plane. Based on the beam diameter (25 $\mu$m) these domains are expected to be of the order of a few microns.

Motivated by the results of PKE measurements, there was a series of attempts to verify the existence of edge currents by searching for stray fields coming out of the surface of $Sr_2RuO_4$ [30–33]. These attempts have, as yet, been unsuccessful. The reason for this is not currently understood, but it may well be due to an efficient screening mechanism which can heavily suppress the effective flux generated by the edge current, since Meissner screening is still applicable. For instance, consider the typical $Sr_2RuO_4$ sample used in most experiments, which is 100s of microns thick along the $c$-axis of the crystal. Meanwhile, the coherence length in that direction is only $\xi_c = 3.3$ nm. Instead of stacking the domains with the same chirality on top of each other, whose edge currents would generate a net magnetic flux (subject to Meissner screening), the condensate could potentially lower its energy by switching its chirality along the $c$-axis over the scale of a few $\xi_c$. By averaging out the net flux threading this vertical stack of domains, the quasi-2-dimensional order parameter could minimise the energy associated with the Meissner screening. However, this would also heavily suppress the external dipole fields which can be detected by scanning-SQUID [30, 31] and scanning-Hall probe [32, 33] measurements.

In summary, from all the $d$-vectors in Table 2.2, the chiral symmetry is the only which can account for the results of $\mu$SR and the PKE experiments, making it by far the most likely candidate amongst the unitary states with a $p$-symmetry. Though, a direct observation of spontaneous edge currents is still lacking. There is however substantial body of transport experiments which support the presence of chiral domains, and the breaking of TRS. Unlike the experiments described above, which rely on measuring the magnetization, transport experiments can probe the non-trivial phase variations produced by the chiral states. This is the subject of Chapter 7.

## REFERENCES

[1] A. P. Mackenzie and Y. Maeno. The superconductivity of $Sr_2RuO_4$ and the physics of spin-triplet pairing. *Reviews of Modern Physics*, 75(2):657, 2003.

[2] A. A. Abrikosov, L. P. Gorkov, and I. E. Dzyaloshinski. Methods of quantum field theory in statistical physics. *Dover Publications*, 1975.

[3] T. Matsubara. A new approach to quantum-statistical mechanics. *Progress of Theoretical Physics*, 14(4):351–378, 1955.

[4] M. Eschrig, T. Löfwander, T. Champel, J. Cuevas, J. Kopu, and G. Schön. Symmetries of pairing correlations in superconductor–ferromagnet nanostructures. *Journal of Low Temperature Physics*, 147(3-4):457–476, 2007.

[5] Y. Tanaka and A. A. Golubov. Theory of the proximity effect in junctions with unconventional superconductors. *Physical Review Letters*, 98(3):037003, 2007.

[6] Y. Tanaka, Y. Tanuma, and A. A. Golubov. Odd-frequency pairing in normal-metal/superconductor junctions. *Physical Review B*, 76(5):054522, 2007.

[7] A. J. Leggett. A theoretical description of the new phases of liquid $^3$He. *Reviews of Modern Physics*, 47(2):331, 1975.

[8] V. Berezinskiĭ. New model of the anisotropic phase of superfluid $^3$He. *JETP Lett*, 20(9):287–289, 1974.

[9] F. Bergeret, A. Volkov, and K. Efetov. Long-range proximity effects in superconductor-ferromagnet structures. *Physical Review Letters*, 86(18):4096, 2001.

[10] F. Bergeret, A. F. Volkov, and K. B. Efetov. Odd triplet superconductivity and related phenomena in superconductor-ferromagnet structures. *Reviews of Modern Physics*, 77(4):1321, 2005.

[11] Y. Maeno, S. Kittaka, T. Nomura, S. Yonezawa, and K. Ishida. Evaluation of spin-triplet superconductivity in $Sr_2RuO_4$. *Journal of the Physical Society of Japan*, 81(1):011009, 2011.

[12] Y. Maeno, H. Hashimoto, K. Yoshida, S. Nishizaki, T. Fujita, J. Bednorz, and F. Lichtenberg. Superconductivity in a layered perovskite without copper. *Nature*, 372(6506):532, 1994.

[13] N. Hussey, A. Mackenzie, J. Cooper, Y. Maeno, S. Nishizaki, and T. Fujita. Normal-state magnetoresistance of $Sr_2RuO_4$. *Physical Review B*, 57(9):5505, 1998.

[14] A. Mackenzie, S. Julian, A. Diver, G. McMullan, M. Ray, G. Lonzarich, Y. Maeno, S. Nishizaki, and T. Fujita. Quantum oscillations in the layered perovskite superconductor $Sr_2RuO_4$. *Physical Review Letters*, 76(20):3786, 1996.

[15] A. Mackenzie, R. Haselwimmer, A. Tyler, G. Lonzarich, Y. Mori, S. Nishizaki, and Y. Maeno. Extremely strong dependence of superconductivity on disorder in $Sr_2RuO_4$. *Physical Review Letters*, 80(1):161, 1998.

[16] A. Mackenzie, S. Julian, A. Diver, G. McMullan, M. Ray, G. Lonzarich, Y. Maeno, S. Nishizaki, and T. Fujita. Quantum oscillations in the layered perovskite superconductor $Sr_2RuO_4$. *Physical Review Letters*, 76(20):3786, 1996.

[17] T. Rice and M. Sigrist. $Sr_2RuO_4$: an electronic analogue of $^3$He ? *Journal of Physics: Condensed Matter*, 7(47):L643, 1995.

[18] K. Ishida, H. Mukuda, Y. Kitaoka, K. Asayama, Z. Mao, Y. Mori, and Y. Maeno. Spin-triplet superconductivity in $Sr_2RuO_4$ identified by $^{17}$O Knight shift. *Nature*, 396(6712):658, 1998.

[19] J. Duffy, S. Hayden, Y. Maeno, Z. Mao, J. Kulda, and G. McIntyre. Polarized-neutron scattering study of the Cooper-pair moment in $Sr_2RuO_4$. *Physical Review Letters*, 85(25):5412, 2000.

[20] J. Jang, D. Ferguson, V. Vakaryuk, R. Budakian, S. Chung, P. Goldbart, and Y. Maeno. Observation of half-height magnetization steps in $Sr_2RuO_4$. *Science*, 331(6014):186–188, 2011.

[21] Y. Yasui, K. Lahabi, M. S. Anwar, S. Yonezawa, T. Terashima, J. Aarts, and Y. Maeno. Half-quantum fluxoid features in the magnetotransport of $Sr_2RuO_4$ micro rings. *Bulletin of the American Physical Society*, 2018.

[22] M. Anwar, S. Lee, R. Ishiguro, Y. Sugimoto, Y. Tano, S. Kang, Y. Shin, S. Yonezawa, D. Manske, H. Takayanagi, et al. Direct penetration of spin-triplet superconductivity into a ferromagnet in au/$SrRuO_3$/$Sr_2RuO_4$ junctions. *Nature Communications*, 7:13220, 2016.

[23] J. F. Annett. Symmetry of the order parameter for high-temperature superconductivity. *Advances in Physics*, 39(2):83–126, 1990.

[24] K. Machida, M.-a. Ozaki, and T. Ohmi. Odd-parity pairing superconductivity under tetragonal symmetry-possible application to $Sr_2RuO_4$. *Journal of the Physical Society of Japan*, 65(12):3720–3723, 1996.

[25] A. P. Mackenzie, T. Scaffidi, C. W. Hicks, and Y. Maeno. Even odder after twenty-three years: the superconducting order parameter puzzle of $Sr_2RuO_4$. *NPJ Quantum Materials*, 2(1):40, 2017.

[26] G. M. Luke, Y. Fudamoto, K. Kojima, M. Larkin, J. Merrin, B. Nachumi, Y. Uemura, Y. Maeno, Z. Mao, Y. Mori, et al. Time-reversal symmetry-breaking superconductivity in $Sr_2RuO_4$. *Nature*, 394(6693):558, 1998.

[27] J. Xia, Y. Maeno, P. T. Beyersdorf, M. Fejer, and A. Kapitulnik. High resolution polar Kerr effect measurements of $Sr_2RuO_4$: evidence for broken time-reversal symmetry in the superconducting state. *Physical Review Letters*, 97(16):167002, 2006.

[28] J. Xia, P. T. Beyersdorf, M. M. Fejer, and A. Kapitulnik. Modified sagnac interferometer for high-sensitivity magneto-optic measurements at cryogenic temperatures. *Applied Physics Letters*, 89(6):062508, 2006.

[29] A. Bouhon and M. Sigrist. Influence of the domain walls on the Josephson effect in $Sr_2RuO_4$. *New Journal of Physics*, 12(4):043031, 2010.

[30] J. Kirtley, C. Kallin, C. Hicks, E.-A. Kim, Y. Liu, K. Moler, Y. Maeno, and K. Nelson. Upper limit on spontaneous supercurrents in $Sr_2RuO_4$. *Physical Review B*, 76(1):014526, 2007.

[31] C. W. Hicks, J. R. Kirtley, T. M. Lippman, N. C. Koshnick, M. E. Huber, Y. Maeno, W. M. Yuhasz, M. B. Maple, and K. A. Moler. Limits on superconductivity-related magnetization in $Sr_2RuO_4$ and $PrOs_4Sb_12$ from scanning SQUID microscopy. *Physical Review B*, 81(21):214501, 2010.

[32] P. J. Curran, V. V. Khotkevych, S. J. Bending, A. S. Gibbs, S. L. Lee, and A. Mackenzie. Vortex imaging and vortex lattice transitions in superconducting $Sr_2RuO_4$ single crystals. *Physical Review B*, 84(10):104507, 2011.

[33] P. Curran, S. Bending, W. Desoky, A. S. Gibbs, S. L. Lee, and A. Mackenzie. Search for spontaneous edge currents and vortex imaging in $Sr_2RuO_4$ mesostructures. *Physical Review B*, 89(14):144504, 2014.